

Influence of physical ageing on the yield response of model DGEBA/poly(propylene oxide) epoxy glasses

Christian G'Sell* and Gregory B. McKenna

National Institute of Standards and Technology, Polymers Division,
Gaithersburg, MD 20899, USA

(Received 23 April 1991; revised 19 July 1991; accepted 8 August 1991)

Cylindrical specimens were prepared from two diglycidyl ether of bisphenol A (DGEBA) amine-terminated poly(propylene oxide) (PPO) networks of different crosslink density and subjected to quenching and isothermal ageing treatments at different temperatures and ageing times of between 0.1 and 1000 h. The changes in the structure of the glasses during the ageing towards equilibrium was subsequently assessed by measurement of the yield stress in uniaxial compression at the same temperature as the ageing. It was found that for both resins, the yield stress increases by as much as 1.8 times over the range of ageing times investigated. It was found for each system that the evolution of the yield stress virtually ceases after a critical ageing time t^* which increases as temperature decreases. Also, it was observed that the lower yield stress corresponding to the onset of generalized plastic flow exhibits only a very small increase with the ageing time. From the influence of temperature and strain rate on the above phenomena, the kinetics of physical ageing were examined quantitatively in terms of the time-ageing time-temperature equivalence principle. The results suggest that the increase in yield stress on ageing is correlated to volume recovery and to the induced increase of the relaxation times as the polymeric glass evolves towards its equilibrium state.

(Keywords: compression; epoxy; glasses; networks; physical ageing; plastic yielding)

INTRODUCTION

It is well known that amorphous polymers exhibit a slow but significant evolution in their mechanical properties after they are quenched from above to below the glass transition temperature, T_g , and then aged isothermally in the glassy state. Since no chemical degradation of the material can be invoked in most cases, such evolution of the properties has come to be called 'physical ageing'^{1,2}. The phenomena reported most extensively in the literature are concerned with the gradual increase of the isochronal viscoelastic modulus due to shifts in the relaxation response as ageing proceeds³⁻⁵, the reduction in the creep rate⁶⁻⁸, the increase of the strength under tension or multi-axial deformation⁹⁻¹² and, to a lesser extent, the decrease of the impact fracture energy of the aged materials^{13,14}. The evolution of the mechanical behaviour has been attributed to changes in thermodynamic properties such as specific volume^{1,2,15-18} or enthalpy as the ageing or annealing time increases^{10,15,19}.

Physical ageing is of considerable practical importance. In the case of engineering parts made of thermoplastic glasses, for example, the initial properties of the material just after the thermomechanical forming process are not stable and will evolve towards a chronologically distant equilibrium during the service life of the parts. More fundamentally, it is essential to characterize quantitatively the physical ageing phenomena in well characterized

materials in order to model the specific microscopic mechanisms which control the observed property evolution. Although many previous papers have shown unambiguously that the effect of physical ageing on the mechanical properties is due to the evolution of the amorphous structure towards a state extrapolated from the liquid structure above T_g down to the actual temperature, many aspects of the problem are still unclear. On one hand, very few works provide a complete set of measurements of the various mechanical responses over a large range of ageing times and temperatures, and the available data are usually insufficient for quantitatively evaluating the ageing kinetics. On the other hand, the precise nature and evolution of the localized molecular motions which control the non-linear viscoelastic response and the yield behaviour need to be determined in more detail.

In this laboratory, an extensive effort was initiated a few years ago to analyse various aspects of physical ageing in model epoxy systems^{3-5,18}. One goal of working with these thermosets was to separate clearly the intrinsic effects of the ageing treatments on the mobility of the chains from other parameters such as molecular weight, degree of entanglement, crystallization, crazing, etc. which may play major roles in thermoplastics. In a recent study, it was shown from viscoelastic experiments in relaxation and creep^{3-5,18} that model diglycidyl ether of bisphenol A (DGEBA)/poly(propylene oxide) (PPO) networks exhibit classical time-ageing time superposition of the viscoelastic responses after a sudden quench from above T_g . The rate of the evolution

*Permanent address: Laboratoire de Physique du Solide (URA CNRS 155), Ecole des Mines, Parc de Saurupt, 54042 Nancy-Cedex, France

towards equilibrium was found to depend primarily on the offset of the ageing temperature T_e with respect to T_g and to be independent of the applied stresses. At that time, it was also found that a time–crosslink density superposition rule could describe the linear viscoelastic behaviour of the same model systems, but that time–stress superposition was not applicable. This prior work was carried out from the linear into the non-linear viscoelastic regime, but below yielding of the polymer.

The present work is focused on the effect of physical ageing on the plastic yielding of two selected resins in the same series as studied previously^{3–5,18}, which exhibit the feature of having the same architecture and flexible chain segments of different length. The yield stress was recorded under compression at two different strain rates at the same temperature as the ageing temperature, T_e . A complete set of results was obtained with both resins as a function of T_e and the ageing time t_e . The results are discussed in terms of the evolution of the structure towards that of the equilibrium glass and with reference to a temperature–ageing time equivalence principle.

MATERIALS AND METHODS

Preparation and characterization of the specimens

The resins investigated were obtained from epoxide-terminated DGEBA (DER 332, Dow Chemical, USA*) cured with an amine-terminated PPO (Jeffamine, Texaco Chemical Company). In this work, two particular amines were considered (namely Jeffamines D400 and D230), which have the same diamine functionality, but differ in their average molecular weight: about 400 g mol^{-1} and 230 g mol^{-1} , respectively. The sample elaboration technique was described in detail elsewhere³. The liquid diepoxy and diamine reagents were stirred in stoichiometric proportions. The homogeneous mixture thus obtained was carefully degassed under vacuum, and cast as plates 12 mm thick. The resin was finally cured in an air oven at 100°C for 24 h.

Under the assumption that the crosslinking reaction corresponds to the opening of the epoxy rings in the presence of the amine groups and that any secondary reaction of the OH groups is negligible, the two resins can be considered as model networks whose structure, represented schematically in *Figure 1*, is constituted of tetrafunctional PPO branches crosslinked at each end with two DGEBA molecules²⁰. Based on the above scheme, it can be readily calculated that the number of rotatable covalent bonds along the macromolecular chains in the network is 10 for the DGEBA branches (not including the two highly hindered bonds within the bisphenol A group), and about 20 or 11 for the PPO branches, depending on the molecular weight of the Jeffamine employed. Although in these networks both the DGEBA and the PPO branches participate in the macromolecular mobility, it is possible that the PPO branches play a major role. This is suggested by results reported previously for the effect of PPO length on the change in the heat capacity, ΔC_p , at the glass transition temperature and ageing in the linear viscoelastic regime

*Certain commercial materials and equipment are identified in this paper to specify adequately the experimental procedure. In no case does such identification imply recommendation or endorsement by the National Institute of Standards and Technology, nor does it imply necessarily that the product is the best available for the purpose

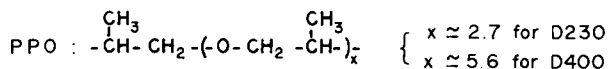
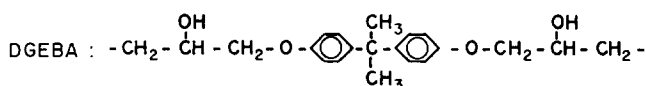
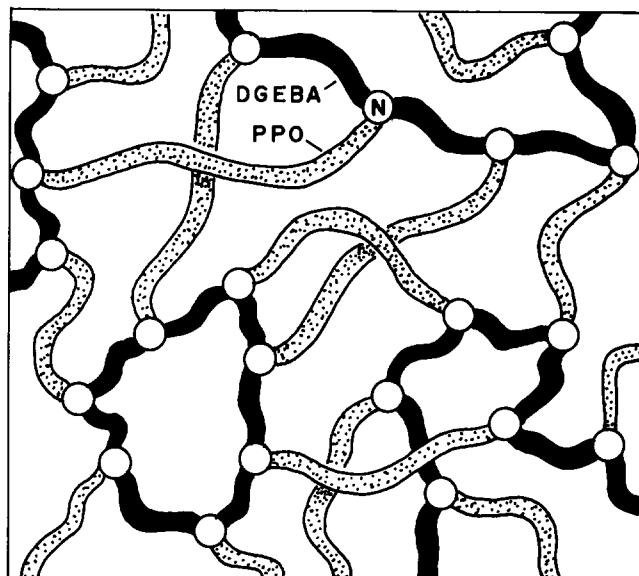


Figure 1 Schematic architecture of the DGEBA/PPO networks. Note that the chemical structures are for the DGEBA and PPO branches between nitrogens only

for the same networks^{3–5}, but requires confirmation in more elaborate studies.

The glass transition temperature of both materials was determined by differential scanning calorimetry (d.s.c.), during heating at $20^\circ\text{C min}^{-1}$ immediately following a cooling at the same rate. The values thus obtained are 42.4°C for the DGEBA + PPO D400 and 87.4°C for the DGEBA + PPO D230. In the present paper, we will occasionally use these temperatures as operational reference points for each material as a means of expressing the ageing temperatures, and they will be noted as T_{ref} rather than T_g . This is because the glass-forming process depends highly on kinetic factors and, as such, is a function of the thermal history of the sample^{2,15}. Correspondingly, the glass transition obtained by d.s.c. measurements is merely conventional since its measured value is that obtained for arbitrarily chosen cooling and heating rates.

Cylindrical specimens were machined out of the cured resin plates with an original length $L_0 = 30 \text{ mm}$ and a diameter $D_0 = 10 \text{ mm}$. Considerable care was taken while machining the samples to obtain very smooth and parallel end surfaces, within 0.02 mm . Visual inspection of all the samples revealed no internal flaws or bubbles.

Thermal treatments

Ageing of the specimens was performed using the following procedure. First, the specimens were subjected to a 'normalization' treatment above T_{ref} (15 h in an oven at 70°C for the DGEBA + PPO D400 or 110°C for the DGEBA + PPO D230). For specimens which had been recycled from a previous compression experiment, heating above T_{ref} let the material completely

recover its original shape, and made possible the use of the same samples for several experiments. This is because the epoxy networks are crosslinked and the normalization brings the resin into a rubber-like state where the chains evolve rapidly to their relaxed configurations of maximum entropy.

After this initial treatment, the specimens were quenched in water baths maintained at the desired ageing temperature T_e with a precision of $\pm 0.2^\circ\text{C}$ and were left at this temperature for an ageing time t_e in the range from 10 min to 42 days (0.17–1000 h). For the normalization, as well as for the ageing treatment which followed, the specimens were kept in small glass ampoules with some dessicant powder. Only for the shortest ageing time (0.17 h) were the specimens taken out of the ampoule and quenched directly into the ageing bath for faster cooling. However, no significant moisture pick-up of the polymer appeared to occur during this short time. Consequently, all the properties described in this paper refer to the dry state of the material.

Compression tests

The yield behaviour of the epoxy glasses was assessed by means of compression tests run at the ageing temperature. This point differs from many previous studies in which tests of yield and failure were performed at a fixed temperature (generally near ambient), which differed from the ageing temperature^{9,10}. The procedure adopted here avoids the problems associated with a second quenching from T_e to the testing temperature.

A special compression system was designed whose most important feature is good temperature control (Figure 2). This was obtained by insulating the ends of the stainless steel compression anvils by means of low-conduction discs, and by controlling the temperature of the sample through a three-action thermal regulation. Not only was the environmental chamber held at the desired temperature with a forced air oven, but also the compression anvils were separately heated by low-intensity resistors with individual temperature regulation

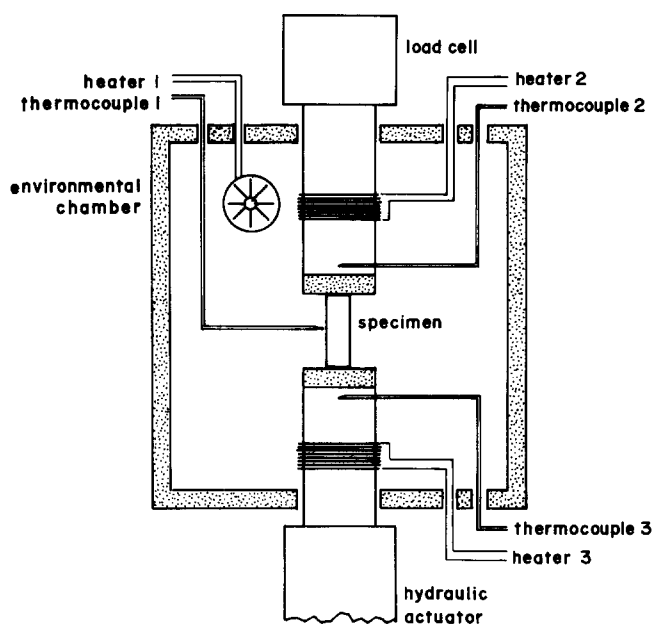


Figure 2 Diagram of the compression cell with thermal regulation systems

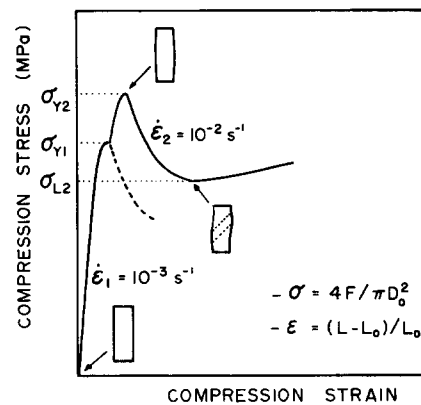


Figure 3 Definition of the parameters for the dual-rate compression experiments

and monitoring. By means of this system, variations of less than $\pm 0.1^\circ\text{C}$ were recorded in time or space in the oven and test fixtures surrounding the samples. The specimen could be placed very rapidly in the compression cell due to the use of an appropriate centring device. Thus temperature changes in the samples during transfer from the ageing bath to the testing machine were minimized.

The compression cell was installed in a servo-hydraulic Instron machine. Because of the low stiffness of the material at the highest experimental temperatures, an extensometer could not be clipped onto the samples at these temperatures. Nevertheless, because of the large size of the compression fixtures, the rigidity of the machine and fixtures was much greater, from six to 15 times, than the rigidity of the samples, so that the 'engineering' strain rate experienced by the specimen was fairly constant for a given crosshead velocity.

The tests were run at a dual strain rate following a procedure that has been successfully applied in previous work²¹. Initially, the compression began at a slow strain rate ($\dot{\epsilon}_1 = 10^{-3} \text{ s}^{-1}$) until the material reached the yield stress σ_{Y1} characteristic of this strain rate (Figure 3). At this moment, just before the stress would normally decrease due to the yielding and strain softening of the material, a strain rate jump was imposed ($\dot{\epsilon}_2 = 10^{-2} \text{ s}^{-1}$) until a second higher yield stress σ_{Y2} corresponding to the new rate was attained. This procedure made possible the assessment of the strain rate sensitivity of the polymer from a single test. In separate tests, we verified that the yield stress obtained at the higher rate is the same as the value determined from a test run entirely at this rate.

For glassy epoxy resins, as in most amorphous polymers below their conventionally measured T_g , the yield stress occurred for a strain of about 3–5%, corresponding to the beginning of a transient plastic regime²². While the deformation in the pre-yield stage was nearly homogeneous, the strain softening regime which follows was associated with the development of localized shear bands, especially at the lowest studied temperatures ($T_{\text{ref}} - T \approx 20^\circ\text{C}$). This resulted in various types of plastic instability, including bulging and kinking. Consequently, the lower yield stress recorded at $\dot{\epsilon}_2$ at the end of the transient regime (noted σ_{L2} in Figure 3) should only be considered cautiously as reflecting the true stress experienced locally by the resin. However, because the value of this minimum engineering stress was found to be unexpectedly reproducible and seems to provide some

complementary information on the effect of physical ageing on the plastic flow regime, we report its variation with ageing along with those of σ_{Y1} and σ_{Y2} .

As noted above, most of the specimens were subjected to several normalization, ageing and compression experiments. These repeat tests were found to be highly reproducible. It was found, for example, that the upper and lower yield stresses obtained after a normalization and a short ageing time were precisely the same (within the narrow experimental error band) irrespective of the fact that the sample was freshly cured or had been subjected before to a 1000 h ageing at any temperature. This kind of observation, reproduced a number of times in this work, clearly indicates that no further chemical changes were occurring due to the multiple thermal treatments and there was no irreversible damage due to the plastic deformation.

RESULTS

Illustration of the effects of isothermal ageing

The stress-strain curves displayed in Figure 4 are typical of the results obtained with the DGEBA + PPO D400 samples held at 27.4°C ($T_{ref} - 15^\circ\text{C}$). They correspond to ageing times of 10 min, 50 min, 7 h, 5 days and 46 days, as indicated. It should be remarked first that the highly non-linear stage preceding the upper yield point exhibits some sensitivity to ageing. Although the compression technique was not specifically designed to assess the viscoelastic properties of the materials, it is evident that the slope in the linear range of the curves increases gradually on ageing. This apparent stiffening is relevant to previous measurements carried out with relaxation techniques³. It corresponds clearly to the decrease of chain mobility as the glassy network evolves

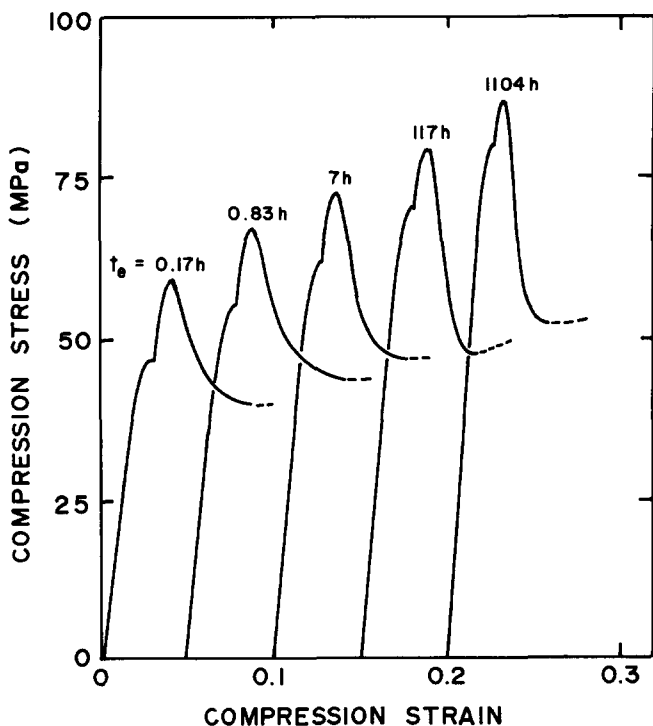


Figure 4 Typical compression curves obtained at $T_e = T_{ref} - 15^\circ\text{C} = 27.4^\circ\text{C}$ for different ageing times in the case of the DGEBA/PPO D400 resin

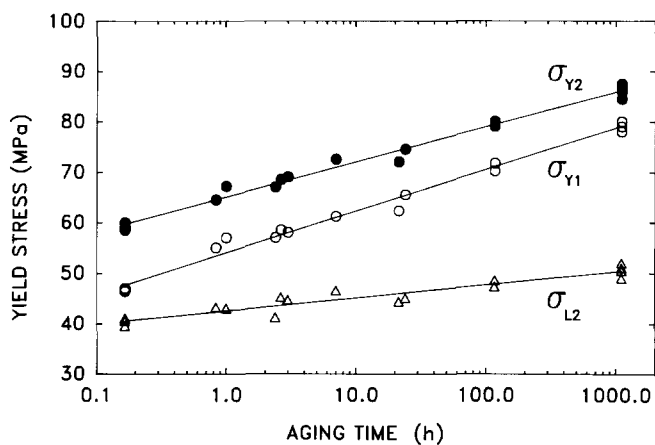


Figure 5 Influence of ageing time on the parameters of the compression tests for the same conditions as in Figure 4

with time towards equilibrium. Also, the curves in Figure 4 show the dramatic increase of the upper yield stress, e.g. σ_{Y1} , from 46.5 MPa for the shortest ageing time of 0.17 h, up to 80 MPa after 1104 h. This represents an increase of 1.72 times in the plastic threshold. After the stress maximum has been reached at σ_{Y1} , the strain rate jump to $\dot{\epsilon}_2$ leads to the second upper yield stress σ_{Y2} which is also observed to increase with t_e , but somewhat more slowly. As a result of this different evolution, the stress jump is less pronounced for the samples having undergone the longest ageing treatments. The last feature investigated in this work is the stress drop following the yield peak at $\dot{\epsilon}_2$ which appears to be more and more abrupt at large t_e , and consequently the lower yield stress, σ_{L2} , increases less on ageing (1.3 times for the longest t_e) than do σ_{Y1} and σ_{Y2} . Also, it was found from visual observation during the tests that the strain inhomogeneities which developed in the samples during the yield drop were confined to narrower zones for the samples aged for longer times.

We now analyse in more detail the kinetics of the ageing process for the same illustrative case (DGEBA + PPO D400, $T_e = T_{ref} - 15^\circ\text{C}$). The curves displayed in Figure 5 show that each of the parameters introduced (σ_{Y1} , σ_{Y2} and σ_{L2}) follows a linear variation versus $\log(t_e)$, with a constant slope from 0.17 to 1104 h. This result correlates clearly with the increasing stiffness of such resins during their service life. From the semilogarithmic plots, it is tempting to predict the effects of physical ageing beyond the limit of the longest time investigated in this work. For example, extrapolating the σ_{Y2} versus $\log(t_e)$ linear regression indicates that the upper yield stress should reach 100 MPa after about 12 years of ageing (88 000 h). However, this prediction is valid only if the ageing kinetics does not slow down in the meantime. This point will be explored in the following section from experiments run at temperatures much closer to the glass transition.

Influence of temperature on the kinetics of ageing

The curves in Figures 6 and 7 correspond to the same type of data as those displayed in Figure 5, but for both resins and at several ageing temperatures. Concerning the plots of the upper yield stresses σ_{Y1} and σ_{Y2} versus $\log(t_e)$ (Figures 6a and b and 7a and b) it is evident that the ageing process does slow down at long times and/or high ageing temperatures. Following a

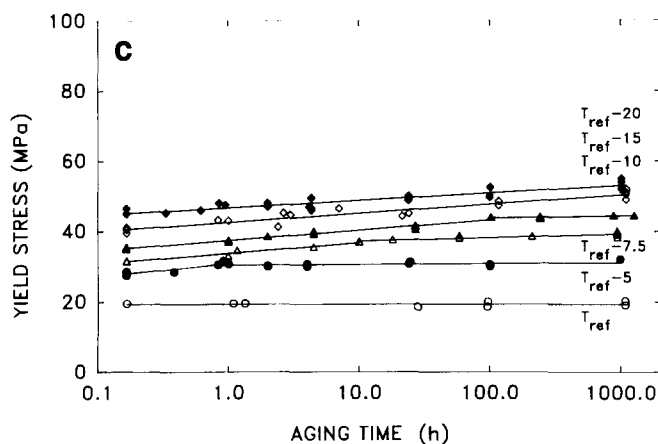
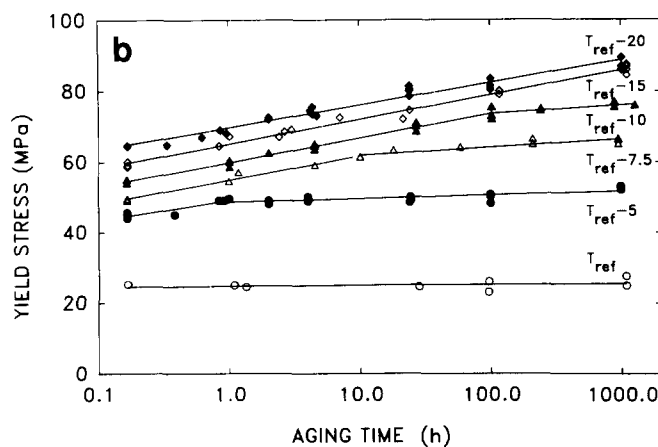
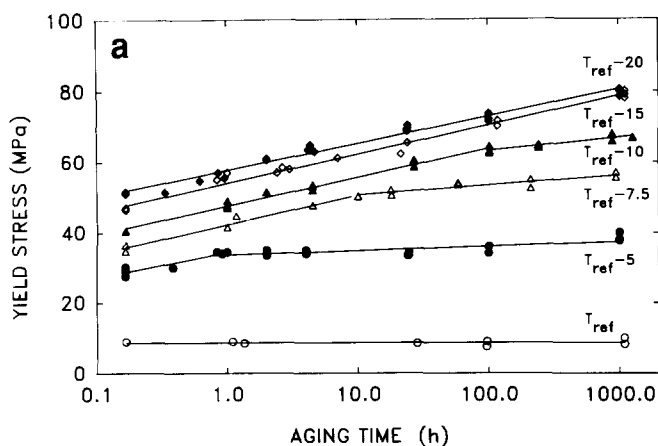


Figure 6 Isothermal ageing curves for the DGEBA/PPO D400 resin : (a) upper yield stress at $\dot{\epsilon} = 10^{-3} \text{ s}^{-1}$; (b) upper yield stress at $\dot{\epsilon} = 10^{-2} \text{ s}^{-1}$; (c) lower yield stress at $\dot{\epsilon} = 10^{-2} \text{ s}^{-1}$

procedure introduced in a previous work³ on the viscoelastic response of epoxies during physical ageing, we analyse the variation of the yield stresses assuming that there are two distinct ageing stages corresponding to short and long times respectively. The transition from fast to slow ageing appears within the experimental time window at temperatures between $T_{ref} - 5^\circ\text{C}$ and $T_{ref} - 10^\circ\text{C}$. In the range of ageing times considered, both stages obey linear regressions on the semilog plots and one obtains directly a measure of the ageing rate $R = [d\sigma_i/d \log(t_e)]_{T_e}$, where σ_i holds for σ_{Y1} , σ_{Y2} and σ_{L2} . The experimental values are reported in Table 1, where R_f is the rate in the fast regime and R_s is the rate in the slow regime. The time t^* at the change from R_f

to R_s is also indicated in the table when appropriate. It does not seem that t^* changes significantly with $\dot{\epsilon}$ but it does vary strongly with T_e : about 0.4 decade $^\circ\text{C}^{-1}$ for the DGEBA + PPO D400 and 0.6 decade $^\circ\text{C}^{-1}$ for the DGEBA + PPO D230.

Several remarks should be made about these data. First, it is interesting that the determination of the parameters of the semilog regression, namely R_f , t^* and R_s , makes possible a reliable prediction of the effects of long-term ageing treatments such as for the specific case of the yield stress prediction at 12 years evoked in the preceding section (DGEBA + PPO D400 at $T_{ref} - 15^\circ\text{C}$). The extrapolated transition time t^* being equal to about 10000 h, one finds that σ_{Y2} would not reach 100 MPa after this 12 year ageing period.

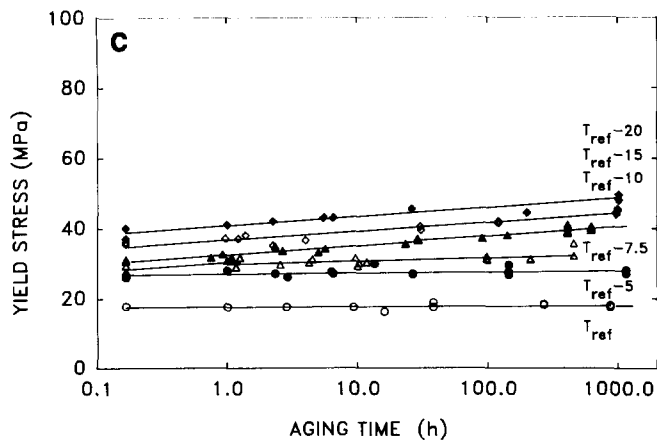
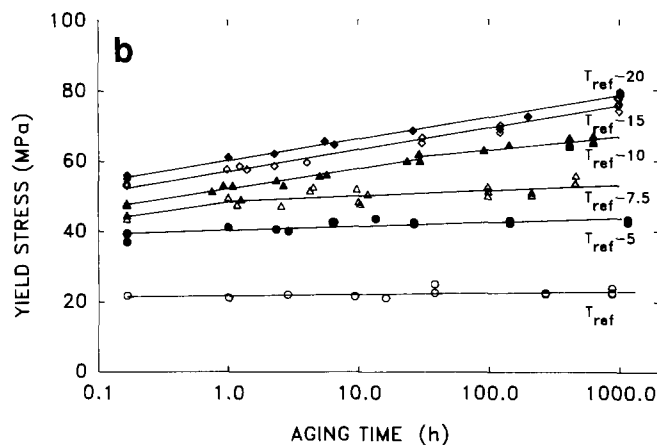
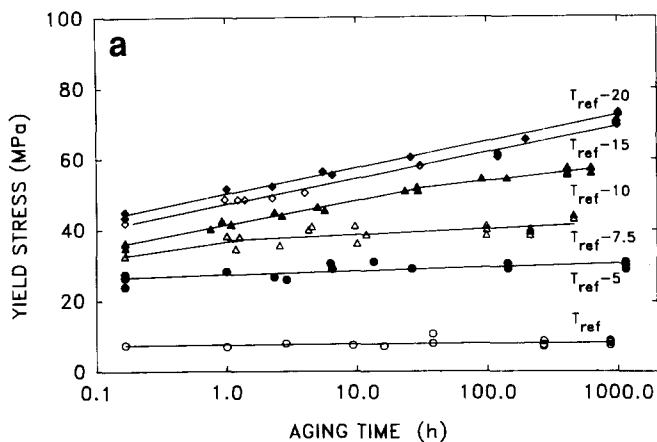


Figure 7 Isothermal ageing curves for the DGEBA/PPO D230 resin : (a) upper yield stress at $\dot{\epsilon} = 10^{-3} \text{ s}^{-1}$; (b) upper yield stress at $\dot{\epsilon} = 10^{-2} \text{ s}^{-1}$; (c) lower yield stress at $\dot{\epsilon} = 10^{-2} \text{ s}^{-1}$

Table 1 Ageing rates R_f/R_s and transition time t^* obtained by semilog regression from the experimental yield stress curves

T_e	R_f/R_s for σ_{Y1} (MPa decade ⁻¹)		R_f/R_s for σ_{Y2} (MPa decade ⁻¹)		R_f/R_s for σ_{L2} (MPa decade ⁻¹)		t^* (h)	
	D400	D230	D400	D230	D400	D230	D400	D230
T_{ref}^a	-/0.0	-/0.2	-/0.2	-/0.4	-/0.0	-/0.2	<0.1	<0.1
$T_{ref} - 5^\circ\text{C}$	7.3/1.2	-/1.1	5.8/1.0	-/1.1	3.7/0.2	-/0.3	≈ 1	<0.1
$T_{ref} - 7.5^\circ\text{C}$	8.3/2.8	5.0/1.6	6.8/2.3	5.3/1.6	3.0/1.0	2.5/0.9	≈ 10	≈ 1
$T_{ref} - 10^\circ\text{C}$	8.1/3.9	6.9/4.0	6.9/2.5	5.7/3.6	2.9/0.7	2.6/2.6	≈ 100	≈ 25
$T_{ref} - 15^\circ\text{C}$	8.2/-	7.3/-	6.9/-	6.2/-	2.6/-	2.6/-	≈ 1000	> 1000
$T_{ref} - 20^\circ\text{C}$	7.6/-	7.4/-	6.4/-	6.1/-	2.1/-	2.6/-	> 1000	> 1000

^a $T_{ref} = 42.4^\circ\text{C}$ for DGEBA + PPO D400 and 87.3°C for DGEBA + PPO D230

In this experimental range, although the temperature has a dramatic effect on the transition time t^* , it does not drastically affect the ageing rates R_f and R_s of the fast and slow regimes considered individually. However, at temperatures far below T_{ref} , the ageing rate eventually decreases. Complementary experiments performed with the DGEBA + PPO D230 resin at $T_{ref} - 65^\circ\text{C}$ (room temperature) have given values of R_f equal to 2.1 and 1.5 MPa decade⁻¹ for σ_{Y1} and σ_{Y2} , respectively.

Another point, already observed for the specific case of Figure 5, is the higher value of the ageing rate at the lower strain rate. On average, the ageing rate at 10^{-2} s^{-1} is 20% higher than the corresponding value at 10^{-3} s^{-1} . This is consistent with the observation in physical ageing experiments in which viscoelastic properties are studied and the apparent rate of ageing is lower at high stress or strain levels^{1,4,5}. The few cases which fail to follow this rule can be suspected to suffer from experimental errors.

As for the lower yield stress σ_{L2} , the experimental plots (Figures 6c and 7c) show that σ_{L2} is only very weakly dependent on the ageing time. Although the relatively higher dispersion of the data for σ_{L2} makes determination of the ageing parameters less reliable, the data can also be analysed with semilog regressions and the transition times t^* are found to be similar to those obtained for σ_{Y1} and σ_{Y2} . Concerning the significance of this effect, it should be noted, from the observation that the previous normalization and ageing sequences have no influence on the current experiment, that the σ_{L2} versus t_e dependence cannot be due to any slow continuation of the network curing. Rather the authors interpret this dependence in the following way. The lower yield stress corresponds to the moment when the shear band or the axisymmetric bulge initiated at the upper yield point begins to propagate steadily along the sample. Therefore the lower yield stress is indirectly sensitive to the structural state of the material elements which are going to be reached by the plastic instability 'wave' and which are still in the pre-yield deformation regime.

DISCUSSION

Having shown how the yield response varies during physical ageing, it is now necessary to proceed towards an understanding of this phenomenon in terms of changes in thermodynamic state or structure of the polymeric glass, i.e. volume or enthalpy recovery. With this in mind, we will first complete the analysis of the experimental data by constructing master curves and isochronal graphs which will help to give a more complete evaluation of

the respective effects of temperature, strain rate and ageing time. We will then compare our results with the corresponding ageing phenomena which affect other properties such as the viscoelastic response. Common features and discrepancies will be critically analysed in view of identifying the microscopic mechanisms which play a role in physical ageing.

Master ageing curves

The influence of strain rate on the upper yield stress is controlled by the viscoelastic and plastic mechanisms in the network. As postulated previously²², the yield point in glassy polymers is observed when the diffuse viscoelastic relaxation processes become insufficient to accommodate the increasing compression strains imposed by the testing machine. At that point, an avalanche of conformational changes occur in microscopic shear domains where high levels of plastic deformation become localized. Crazing is sometimes an alternative mechanism but it should not be invoked here since it seems to be restricted to thermoplastics and it does not occur in compression. The total deformation rate, $\dot{\epsilon}$, of the epoxide glass is the sum of the viscoelastic rate and the plastic rate. Consequently, when the strain rate is suddenly changed from $\dot{\epsilon}_1$ to $\dot{\epsilon}_2$, less time is allowed to the chain for their viscoelastic relaxation and in order for yield to occur the plastic processes must be activated faster. Thus an increment of stress from σ_{Y1} to σ_{Y2} is required. The less the 'viscoelastic deformability' of the network, the higher the upper yield stress. Finally it is reasonable to account for the effect of time, temperature and ageing time on the yield stress by a similar equivalence principle as for viscoelastic data. Consequently, decreasing the temperature or increasing the ageing time have an equivalent effect on the yield stress as does increasing the strain rate.

According to this time-ageing time-temperature correspondence principle, and modifying the classical procedure¹, we have constructed the master curves for each material (Figure 8). Taking for example the DGEBA + PPO D400, the segments plotted on the left side of Figure 8a are actual data points (only averaged with the semilog regression procedure introduced earlier) corresponding to a selection of ageing times and temperatures for the two strain rates applied. These segments, and those obtained at the other temperatures, were translated horizontally by an appropriate shift factor $\log(a_{T_e, t_e})$. The result of the shifting is the master curve shown in the graph. It should be noted that, for a given experiment at fixed ageing time and temperature,

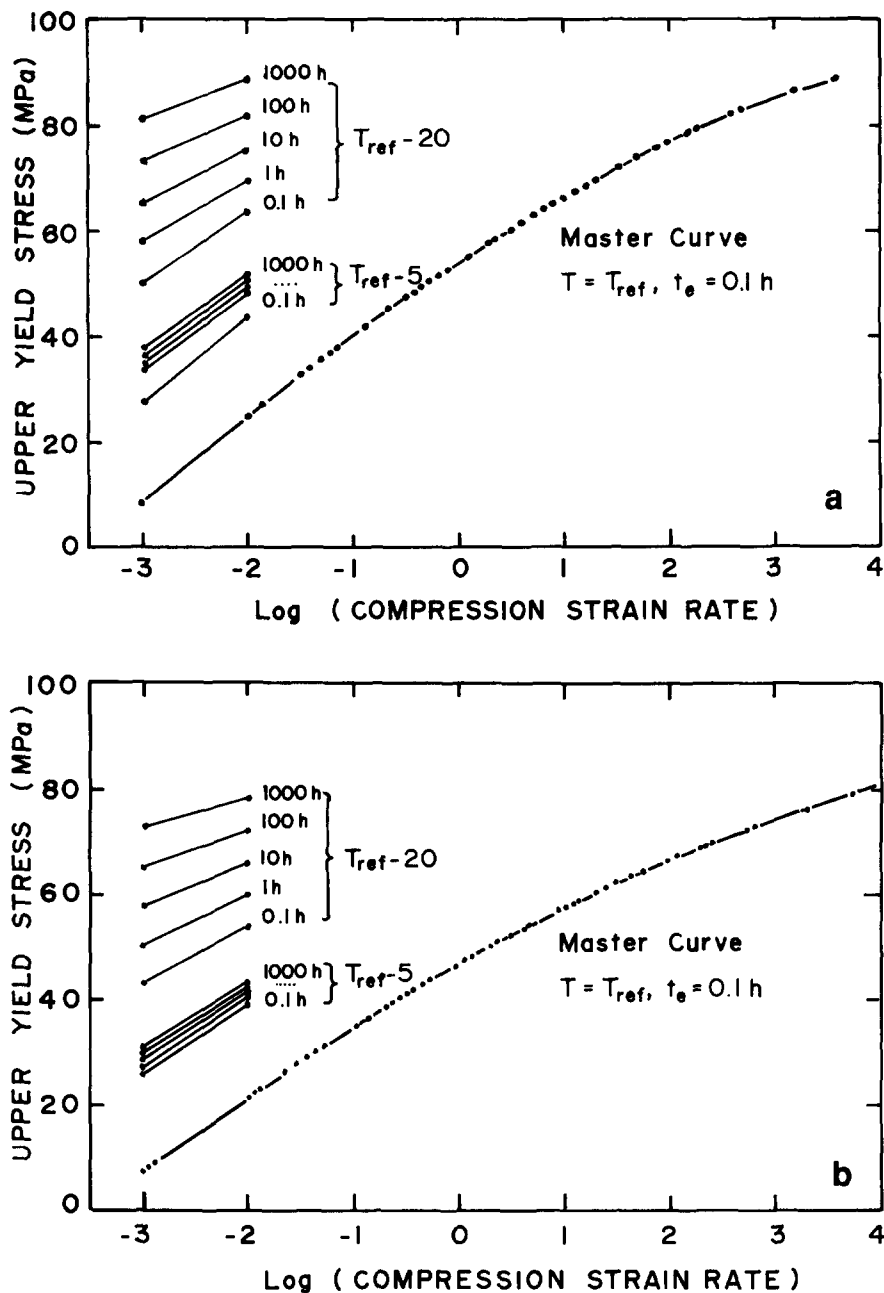


Figure 8 Construction of a master curve by application of the time-ageing time-temperature superposition principle to the upper yield stress versus strain rate curves: (a) for DGEBA + PPO D400; (b) for DGEBA + PPO D230

the shift factor is a function of both parameters. The respective contributions of T_e and t_e on $\log(a_{T_e, t_e})$ can be separated by the following decomposition. Consider, for example, the stack of segments for $T_e = 22.4^\circ\text{C}$ in *Figure 8a*. The construction of the master curve is obtained by the addition of two complementary shifts. First the whole stack is translated horizontally to the right until the segment for the reference ageing time $t_e = 0.1$ h reaches the master curve. This shift is noted $\log(a_{T_e})$. Then the different segments in the stack are individually shifted to the right until they fit the master curve. This second shift is noted $\log(a_{t_e})$. The total shift is then $\log(a_{T_e, t_e}) = \log(a_{T_e}) + \log(a_{t_e})$. Both contributions are plotted in *Figure 9a* for the case of DGEBA + PPO D400. Particular attention should be paid to the $\log(a_{t_e})$ component. One notes at short ageing times that all the curves superimpose on the same line

whose slope $[d \log(a_{T_e})/d \log(t_e)]_{T_e}$ is between 0.5 and 1.0. This is because the intrinsic effect of T_e was separately taken into account in the $\log(a_{T_e})$ shift. The transition time t^* appears again on this plot at the time corresponding to the sudden decrease of the slope to a value between 0.1 and 0.2. As stated previously¹⁻³, the advantage of such a representation is that $\log(a_{t_e})$ is a non-dimensional variable which allows one to compare ageing phenomena related to different kinds of material properties. Two interesting observations can be made from *Figures 8b* and *9b*. First the $\log(a_{t_e})$ versus $\log(t_e)$ plots show a curvature which is not observed when viscoelastic shift factors are presented in this way. This result perhaps reflects the differences between the viscoelastic and plastic processes and the influence of the physical ageing 'thermodynamic' evolution on them. Second, the values of t^* at which there is an abrupt

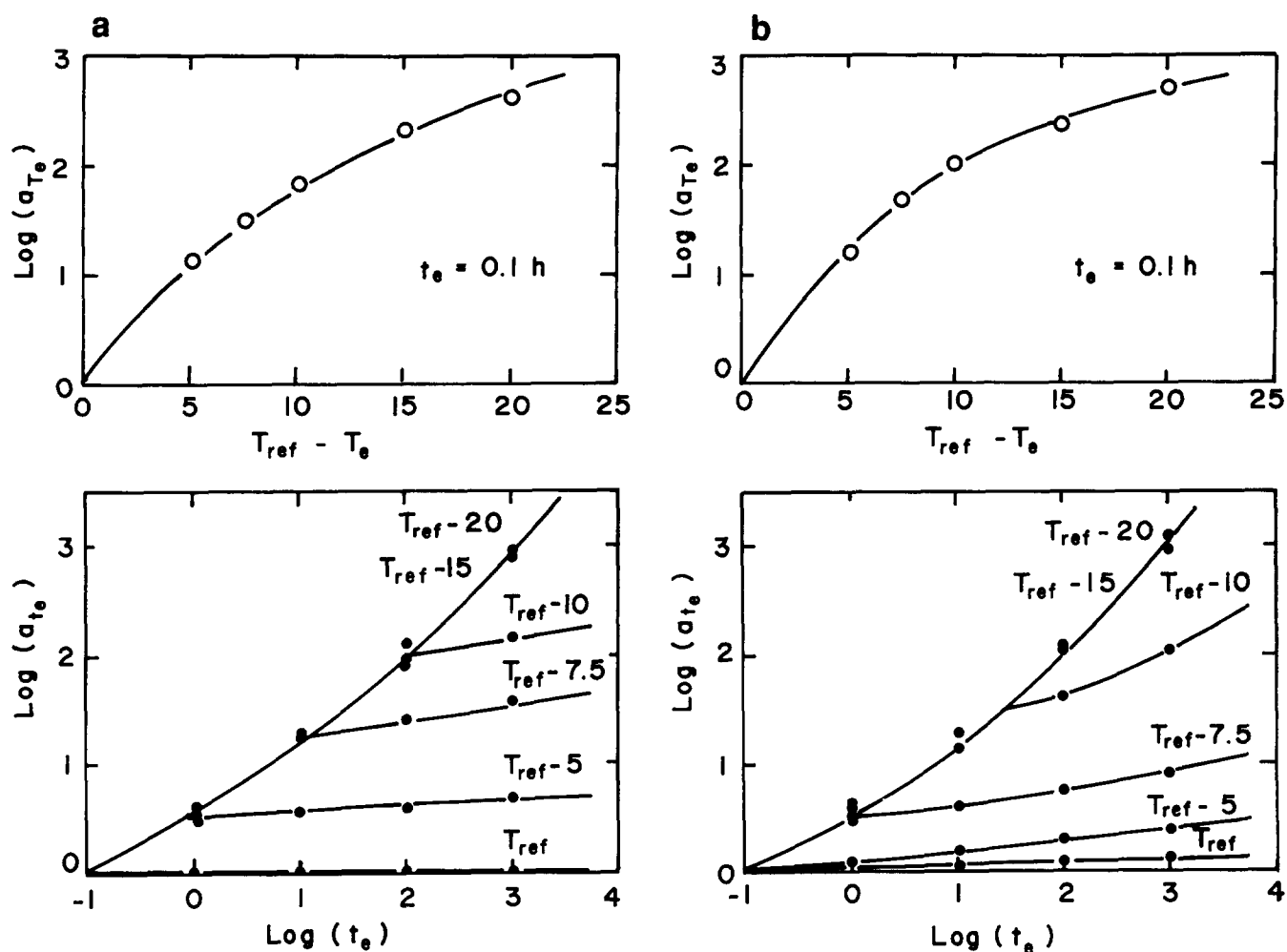


Figure 9 Shift factors for the master curves of Figure 8 (for the definition of $\log(a_{T_e})$ and $\log(a_{t_e})$, see text): (a) for DGEBA + PPO D400; (b) for DGEBA + PPO D230

change in slope from an 'ageing' to a 'non-ageing' regime are significantly greater than those obtained previously from viscoelastic measurements^{3-5,18,23,24}. This will be discussed subsequently.

Isochronal ageing curves

As shown in the Experimental section, temperature is one major factor in the plastic processes reported here since it controls the time t^* at which ageing appears to slow down. In order to highlight this effect, Figure 10 shows the isochronal variations of σ_{Y2} versus T_e for each resin. If one considers, for example, the curve for the DGEBA + PPO D400 at $t_e = 10$ h, it is evident that, as temperature decreases, the yield stress increases in three successive steps. First, at high temperatures, the value of σ_{Y2} is practically zero. At about $T_{\text{ref}} + 5^\circ\text{C}$, the yield stress exhibits a dramatic upturn and begins to follow a curve with a steep slope of about $5 \text{ MPa } ^\circ\text{C}^{-1}$. This rise is observed until $T_{\text{ref}} - 10^\circ\text{C}$, at which temperature the isochronal curve branches abruptly towards a much weaker slope of about $1 \text{ MPa } ^\circ\text{C}^{-1}$. This new regime continues to the lowest temperatures investigated. The dashed line labelled $\sigma_{Y2}(t^*)$ is the envelope of the points corresponding to $t^*(T)$ for the different ageing temperatures. Obviously this curve does not represent the yield stress of a glass fully in equilibrium since the ageing continues to proceed slowly after t^* . However, it is unrealistic to expect that the yield stress would grow

indefinitely with the ageing time. Rather, it is likely that the slow rate R_s measured after t^* is the zero-order term of a more complex rate function which tends towards an asymptotic value $\sigma_{Y2}(\infty)$. Since t^* announces the attainment of the equilibrium state of the glass, it is probable that $\sigma_{Y2}(\infty)$ is not much higher than $\sigma_{Y2}(t^*)$. At the present stage of the discussion, we assume that $\sigma_{Y2}(\infty)$ is given qualitatively by the extrapolation of the values of σ_{Y2} at $t_e = 10^5$ h from temperatures close to T_{ref} . This construction is illustrated by the dotted lines in Figures 10a and b.

The isochronal representation is interesting in several respects. First, it illustrates fairly well the kinetic nature of the glass transition temperature. For a given ageing time, we can define $T_g(t_e)$ as the temperature at which the isochronal curve changes slope. In the case of the DGEBA + PPO D400, for example, the T_g thus defined is in the range from about $T_{\text{ref}} - 2.5^\circ\text{C}$ for $t_e = 10^{-1}$ h to about $T_{\text{ref}} - 10^\circ\text{C}$ for $t_e = 10^3$ h. Also of interest is use of the isochrones as a measure of the evolution of a sample during a typical heat treatment, provided the yield stress can be taken as a good indicator of the structural state of the glass. Let us consider, for example, the case of a quench at $T_{\text{ref}} - 20^\circ\text{C}$ from $T_{\text{ref}} + 15^\circ\text{C}$. The continuous cooling experienced by the polymer can be decomposed in a series of successive ageing increments for very short times at successively decreasing temperatures. In the isochronal plot, the path representative of

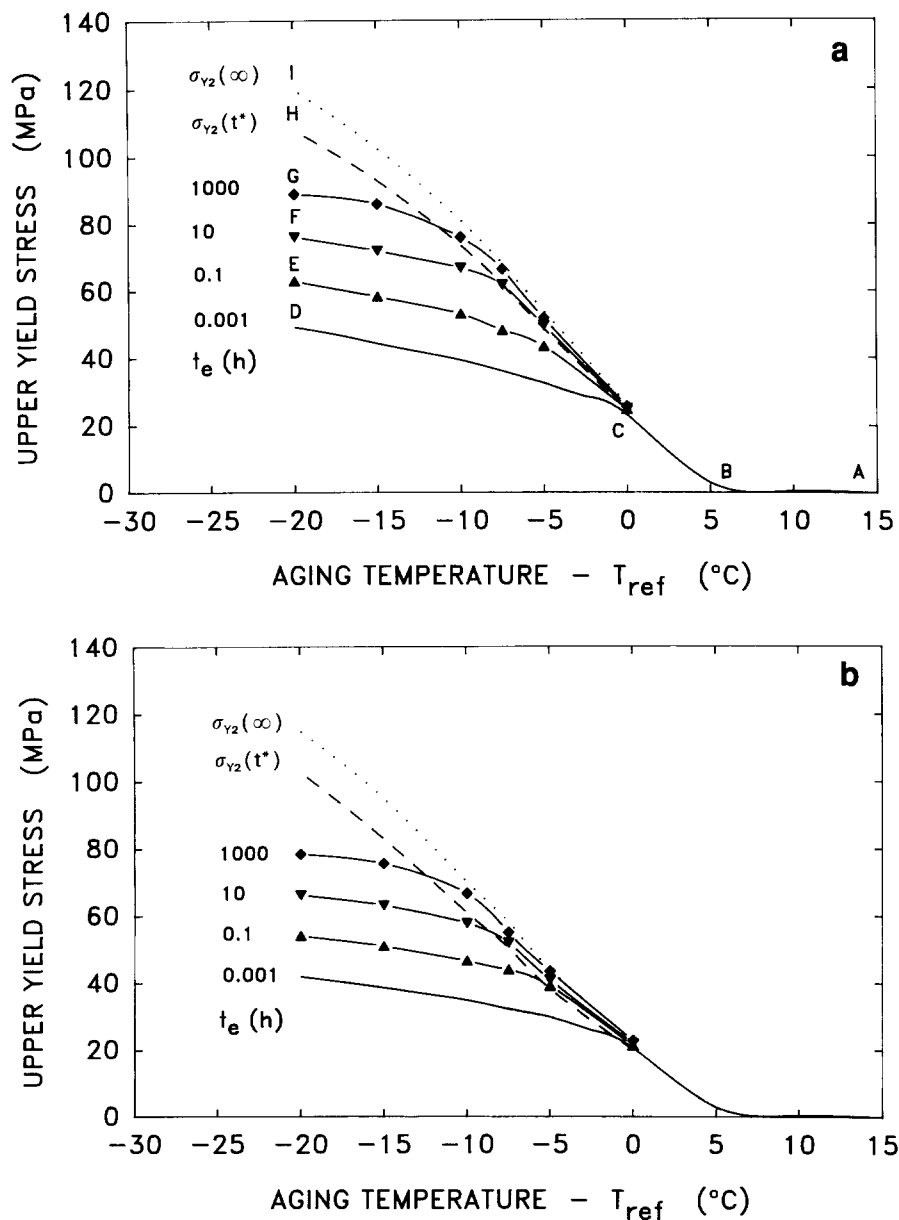


Figure 10 Isochronal ageing curves of the upper yield stress σ_{y2} : (a) for DGEBA + PPO D400; (b) for DGEBA + PPO D230

the quench would be near the line ABCD (Figure 10a) corresponding to a very short t_e , say 0.001 h. After that, if the sample stays immersed in the bath at $T_{ref} - 20^\circ\text{C}$, the representative path would be the vertical isotherm (DEFGHI). It is clear from the graph that the structural evolution would be fast at short immersion times, until reaching the $\sigma_{y2}(t^*)$ curve at point H. It would then slow down more and more while approaching the equilibrium state at point I. This is related to the well known autoretardation in temperature jump experiments (down quench) described by Kovacs¹⁵ in his studies of volume recovery.

Comparison with other ageing phenomena

In this work, we have focused attention on the yield stresses. However, most polymer properties are affected by the time elapsed after quenching. We will examine in this section how the ageing of viscoelastic relaxation³⁻⁸ and volume recovery¹⁵⁻¹⁸ compare with the ageing of the yield behaviour.

In a series of papers on the relaxation and creep behaviour of the same epoxy resins as those studied here³⁻⁵, the ageing of the non-linear viscoelastic response of the networks has been analysed in terms of the time-ageing time-temperature superposition principle. The shift factor curves $\log(a_{t_e})$ versus $\log(t_e)$ which were thus obtained exhibit the same features as the curves in Figure 8: for short t_e all the curves for different T_e values superimpose (with a slope between 0.5 and 1) and they diverge successively into branches of much lower slope. This indicates similar behaviours for the plastic yield mechanisms and the viscoelastic properties. In previous work^{22,25,26}, a model was proposed in which the onset of plastic deformation is achieved by the activation of microscopic shear domains limited by a closed line of strain singularity between the heavily deformed domains and the otherwise viscoelastic matrix. These defects are more or less similar to dislocation loops and their misfit energy increases as the modulus of the matrix increases. Therefore, it is likely that the stiffening of the resin during

ageing would make the activation of the shear domains more difficult and consequently would induce a rise in the yield stress. However, this interpretation is only qualitative. For one thing, the transition time t^* observed by Lee and McKenna³⁻⁵ and Santore *et al.*^{18,23,24} is shorter by one order of magnitude for the viscoelastic modulus than is that for the plastic yield stress measured here. This result suggests that the structural rearrangements which take place during the ageing affect more directly the rather diffuse, viscoelastic relaxation mechanisms than the very local yield processes. The latter are certainly influenced by the viscoelastic stiffening but they seem to be delayed to some extent.

As for the specific volume, it is well established that quenched amorphous polymers are not in thermodynamic equilibrium^{2,15-18,27} and that their volume is larger than can be expected through an extrapolation from the rubber-like state above T_g . Whatever the model or the terminology used to describe the excess volume (free volume, distribution of holes, thermal density fluctuations, etc.) it is clear that the structural recovery that makes the ageing glass evolve toward thermodynamic equilibrium is accompanied by a progressive densification of the material. This phenomenon is active in all glass-forming systems, including thermoplastic and crosslinked polymers. In many cases, the kinetics of volume recovery have been represented by means of isochronal graphs as a function of T_e for fixed values of t_e ^{2,15-17}. It is remarkable how similar the graphs of the isochronal representation of the yield stress (Figure 10) are to those for volume recovery. This similarity constitutes a strong indication that the yield process depends on the excess volume in the non-equilibrium structure. In the shear domain model quoted earlier^{22,25,26}, the effect of the ageing densification can be taken into account as well, since it is likely that the local molecular jumps which control the nucleation and growth of the shear domains are facilitated by the presence of 'holes' in the neighbouring network. Reciprocally, a gradual densification of the network makes the chain motions necessary to accommodate the segmental chain jumps more difficult.

More quantitatively, it is interesting to compare our yield stress results to the thermal volume recovery measurements obtained recently with the DGEBA + PPO D400 by means of a mercury dilatometer¹⁸. In the case of quench to 33.5°C ($T_{ref} - 8.9^\circ\text{C}$), it was shown in Figure 5a of that work that the volume decrease initially exhibits a fast rate ($d \log V / d \log t \approx 5 \times 10^{-4}$ per decade) before slowing down and eventually reaching an asymptotic value after about 100 h. This time is about 1.5 decade longer than our transition time t^* for this rate of ageing temperatures. This appears to confirm that the slow yield stress evolution after t^* is actually the sign of the approaching attainment of equilibrium. It further adds to the time scales which seem to be associated with ageing, e.g. the viscoelastic t^* , the yield t^* and the volume recovery t^* , as discussed by Santore *et al.*^{23,24}.

From the various points of view presented above, it appears that the excess volume and the viscoelastic modulus play complementary roles in the yield process of non-equilibrium resins, although the time scales of their individual responses do not seem to be identical. It is interesting to call attention to a recently published model^{17,30}, based on the elimination of microscopic 'holes' when the polymer temperature is decreased. In

the case of a non-equilibrated glass, the model predicts that a linear relation should exist between the excess volume and the yield stress (which supposedly occurs when the product of the applied strain and the apparent volume retardation time reaches the order of unity). It is thus found that, on ageing, the excess volume decays with time following a stretched exponential function in terms of a characteristic time τ : $\delta(T_e, t_e) = \delta_0 \exp[-(t_e/\tau)^\beta]$, where β defines the shape of the hole energy spectrum. Consequently, the yield stress function should be of the type: $\sigma_Y = \sigma_{Y_0} + \Delta\sigma \{1 - \exp[-(t_e/\tau)^\beta]\}$. It is interesting to remark that this relation is similar to the so-called Kohlrausch-Williams-Watts (KWW) equation frequently utilized to represent broad-spectrum relaxation phenomena^{28,29}. We have used this function to fit our experimental yield stress data in a typical case of the ageing of the DGEBA + PPO D400 at $T_{ref} - 7.5^\circ\text{C}$ (Figure 11). Although the KWW function does not present any slope discontinuity, it exhibits a kind of rounded-off inflexion which fits fairly well the experimental evolution of σ_{Y2} versus $\log(t_e)$ provided appropriate values of the parameters ($\sigma_{Y_0} = 36$ MPa, $\Delta\sigma = 30$ MPa and $\beta = 1/3$) are selected. In this paper, we will not discuss this fit further, since we still lack detailed data for the volume recovery, and therefore cannot fully judge the relevance of the fitted parameters, although the value of $\beta = 1/3$ is similar to that frequently found to describe the mechanical relaxation and creep of glasses^{1,3-5}.

CONCLUSIONS

Two DGEBA + amine-terminated PPO networks with different crosslink density were subjected to quenching and subsequently aged at various temperatures, T_e , over nearly four decades of ageing time, t_e . The yield behaviour was assessed by compression tests at the same temperature as the ageing. The conclusions from these experiments were as follows.

1. There is a considerable increase of the upper yield stress (up to 1.8 times) on ageing from 0.1 to 1000 h.
2. The ageing rate of the upper yield stress is initially rapid before a transition time t^* at which it slows down rather abruptly before tending to a presumably asymptotic limit at very long ageing times.
3. The transition time t^* is shifted to higher values as the ageing temperature is decreased (about 0.4 decade $^\circ\text{C}^{-1}$ for the DGEBA + PPO D400 and 0.6 decade $^\circ\text{C}^{-1}$ for the DGEBA + PPO D230).
4. The ageing of the yield behaviour seems to be closely related to the evolution of the specific volume as the network evolves towards thermodynamic equilibrium.
5. The yield behaviour is influenced by the viscoelastic response. However, the physical ageing seems to affect the viscoelastic response differently than the yield response since the t^* of the yield stress appears to be larger, by one order of magnitude, than the t^* from the viscoelastic measurements found by Lee and McKenna for the same epoxies³⁻⁵. Furthermore, both t^* values occur at times shorter than those required to reach equilibrium in volume recovery experiments.
6. The lower yield stress is not so much influenced by the ageing time, suggesting that the microscopic mechanisms controlling the plastic flow processes are somewhat independent of the prior thermomechanical history.

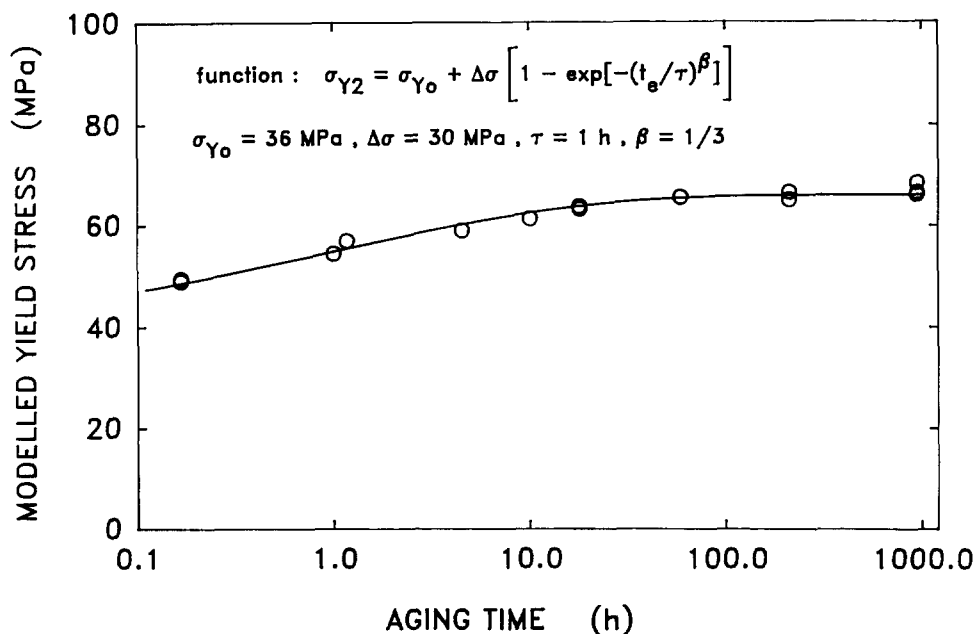


Figure 11 Comparison of a stretched exponential function to the yield stress versus ageing time data for the case of DGEBA + PPO D400 at $T_{\text{ref}} = -7.5^\circ\text{C}$

ACKNOWLEDGEMENTS

This work was done during the sabbatical leave of C.G. at the National Institute of Standards and Technology. He is grateful to this Institute for providing a guest scientist position and to the NATO administration for a special fellowship.

REFERENCES

- 1 Struik, L. C. E. 'Physical Aging in Amorphous Polymers and Other Materials', Elsevier, Amsterdam, 1978
- 2 McKenna, G. B., in 'Comprehensive Polymer Science', Vol. 2 'Polymer Properties' (Eds C. Booth and C. Price), Pergamon, Oxford, 1989
- 3 Lee, A. and McKenna, G. B. *Polymer* 1988, **29**, 1812
- 4 Lee, A. and McKenna, G. B. *Polym. Eng. Sci.* 1990, **30**, 431
- 5 Lee, A. and McKenna, G. B. *Polymer* 1990, **31**, 423
- 6 Read, B. E., Tomlins, P. E. and Dean, G. D. *Polymer* 1990, **31**, 1204
- 7 Ender, D. H. *J. Macromol. Sci. Phys.* 1970, **B4**, 635
- 8 Crissman, J. M. and McKenna, G. B. *J. Polym. Sci., Polym. Phys. Edn* 1990, **28**, 1463
- 9 Golden, J. H., Hammant, B. L. and Hazell, E. A. *J. Appl. Polym. Sci.* 1967, **11**, 1571
- 10 Golden, J. H., Hazell, E. A. and Wright, H. *J. Appl. Polym. Sci.* 1968, **12**, 1385
- 11 Bubeck, R. A., Bales, S. E. and Lee, H. D. *Polym. Eng. Sci.* 1984, **24**, 1142
- 12 Morgan, R. J. *J. Appl. Polym. Sci.* 1979, **23**, 2711
- 13 Mininni, R. M., Moore, R. S., Flick, J. R. and Petrie, S. E. B. *J. Macromol. Sci. Phys.* 1973, **B8**, 342
- 14 McKenna, G. B., Crissman, J. M. and Lee, A. *Polym. Prepr.* 1988, **29**, 128
- 15 Kovacs, A. J. *Fortsch. Hochpolym. Forsch.* 1963, **3**, 394
- 16 Lagasse, R. R. and Curro, J. G. *Macromolecules* 1982, **15**, 1559
- 17 Chow, T. S. *J. Polym. Sci., Polym. Phys. Edn* 1987, **25**, 137
- 18 Santore, M. M., Duran, R. S. and McKenna, G. B. *Polymer* 1991, **32**, 2377
- 19 Berens, A. R. and Hodge, I. M. *Macromolecules* 1982, **15**, 756
- 20 Dusek, K., Ilavsky, M., Stokrova, S., Matejka, L. and Lunaka, S. in 'Crosslinked Epoxies' (Eds B. Sedlacek and J. Kahovec), Walter de Gruyter, Berlin, 1987, p. 279
- 21 Pink, E. *Mater. Sci. Eng.* 1976, **23**, 275
- 22 G'Sell, C. and Jonas, J. *J. Mater. Sci.* 1981, **16**, 1956
- 23 Santore, M. M., Duran, R. S. and McKenna, G. B. Materials Research Society Proceedings, Boston, MA, November 1990
- 24 Santore, M. M. and McKenna, G. B. *J. Non-Crystalline Solids* 1991, **131**, 497
- 25 G'Sell, C. in 'Strength of Metals and Alloys' Vol. 3 (Ed. H. J. McQueen), Pergamon Press, Oxford, 1986, p. 1946
- 26 G'Sell, C., El Bari, H., Perez, J. Cavallé, J. Y. and Johari, G. P. *Mater. Sci. Eng.* 1989, **A110**, 223
- 27 Robertson, R. E. *J. Polym. Sci., Polym. Phys. Edn* 1979, **17**, 597
- 28 Kohlrausch, R. *Ann. Phys. (Leipzig)* 1847, **21**, 393
- 29 Williams, G. and Watts, D. C. *Trans. Faraday Soc.* 1970, **66**, 80
- 30 Chow, T. S. *J. Rheol.* 1986, **30**, 729